AJNR

Comparison of 3D FLAIR, 2D FLAIR, and 2D T2-Weighted MR Imaging of Brain Stem Anatomy

M. Kitajima, T. Hirai, Y. Shigematsu, H. Uetani, K. Iwashita, K. Morita, M. Komi and Y. Yamashita

AJNR Am J Neuroradiol published online 19 January 2012
http://www.ajnr.org/content/early/2012/01/19/ajnr.A2874

Published January 19, 2012 as 10.3174/ajnr.A2874

ORIGINAL RESEARCH

M. Kitajima
T. Hirai
Y. Shigematsu
H. Uetani
K. Iwashita
K. Morita
M. Komi
Y. Yamashita

Comparison of 3D FLAIR, 2D FLAIR, and 2D T2-Weighted MR Imaging of Brain Stem Anatomy

BACKGROUND AND PURPOSE: Although 3D FLAIR imaging visualizes detailed structures of the brain stem, it has not been used to evaluate its normal anatomy. The purpose of this study was to evaluate whether 3D FLAIR images can provide more detailed anatomic information of the brain stem than 2D FLAIR and 2D T2WI.

MATERIALS AND METHODS: We prospectively evaluated MR images in 10 healthy volunteers. 3D and 2D FLAIR images, 2D T2WI, and DTI were obtained on a 3T MR imaging scanner. A VISTA technique was used for 3D FLAIR imaging. White matter tracts and nuclei of the brain stem were determined on 3D and 2D FLAIR images and 2D T2WI by referring to anatomic atlases and DTI color maps. The subjective assessment of the visibility by using a 4-point grading system and the contrast ratio of the structures on 3D and 2D FLAIR images and 2D T2WI were evaluated.

RESULTS: The visibility of the SCP and MCP, DSCP, CST, and CTT was higher on 3D FLAIR images than on 2D T2WI and 2D FLAIR images. The contrast ratio for the CST, SCP, MCP, DSCP, and CTT was significantly different on 3D FLAIR images and 2D T2WI and on 3D FLAIR and 2D FLAIR images; there was no significant difference in contrast ratio for the SCP at the pons on 3D FLAIR and 2D T2WI.

CONCLUSIONS: 3D FLAIR images provide detailed anatomic information of the brain stem that cannot be obtained on 2D T2WI and 2D FLAIR images.

ABBREVIATIONS: CST = corticospinal tract; CTT = central tegmental tract; DSCP = decussation of the superior cerebellar peduncle; MCP = middle cerebellar peduncle; ML = medial lemniscus; RN = red nucleus; SCP = superior cerebellar peduncle; SENSE = sensitivity encoding; SI = signal intensity; SN = substantia nigra; VISTA = volume isotropic turbo spin-echo acquisition

3D FLAIR imaging is a useful technique for evaluating several central nervous system and inner ear diseases.[1-3] Among techniques proposed for obtaining 3D FLAIR images, the VISTA technique is a new 3D TSE sequence that can be used for FLAIR imaging at isotropic high spatial resolution with a high signal intensity–to-noise ratio. VISTA features short echo spacing optimized for a very long echo train readout; this makes it possible to collect all data with fewer TRs. By using the novel technique of refocusing flip angle modulation, VISTA constrains relaxation during the long readout and avoids the blurring commonly associated with long echo trains. In addition, the VISTA technique on 3D FLAIR reduces pulsation and blood flow artifacts.[4]

The brain stem is involved in a number of neurodegenerative disorders such as Alzheimer, Parkinson, and Huntington diseases; typically these have been imaged with T1WI, T2WI, T2*-weighted, and susceptibility-weighted imaging.[5] DTI depicts detailed structures of the brain stem and is also useful for evaluating neurodegenerative disorders.[6,7] Although 3D FLAIR imaging visualizes detailed structures of the brain stem, it has not been used to evaluate its normal anatomy, to our knowledge.

Received July 4, 2011; accepted after revision August 11.

From the Department of Diagnostic Radiology (M.K., T.H., Y.S., H.U., K.I., Y.Y.), Graduate School of Medical Sciences, Kumamoto University, Kumamoto, Japan; and Department of Radiology (K.M., M.K.), Kumamoto University Hospital, Kumamoto, Japan.

Paper previously presented at: 19th Annual Meeting and Exhibition of the International Society for Magnetic Resonance in Medicine, May 6–13, 2011; Montreal, Quebec, Canada.

Please address correspondence to Mika Kitajima, MD, Department of Diagnostic Radiology, Graduate School of Medical Sciences, Kumamoto University, 1–1-one Honjo, Kumamoto, Japan 860-8556; e-mail address: kmikarin@rr.iij4u.or.jp

http://dx.doi.org/10.3174/ajnr.A2874

The purpose of this study was to evaluate the brain stem anatomy on 3D FLAIR images to identify brain stem structures, including the nuclei and white matter tracts and to compare these with findings obtained by DTI, 2D FLAIR, and 2D TSE T2WI.

Materials and Methods

Imaging Protocol

Informed consent was obtained from all subjects; our study protocol was approved by our institutional review board. All scans were obtained on a 3T MR imaging scanner (Achieva; Philips Healthcare, Best, the Netherlands) by using an 8-channel array head coil. Ten healthy subjects (7 men, 3 women; age range, 23–46 years; mean, 35.0 years) underwent whole-brain MR imaging including 3D and 2D FLAIR imaging, 2D T2WI, and DTI. A volume isotropic TSE acquisition (VISTA) technique, comprising a 3D TSE sequence by using a nonselective refocusing pulse and refocusing control, was used for 3D FLAIR imaging. The parameters for 3D FLAIR imaging were the following: TR/TE, 8000/355 ms; TI, 2400 ms; turbo factor, 110; refocusing angle; 50°; spatial resolution, 1 × 1× 2 mm; reconstructed resolution, 1 × 1 × 1 mm; and SENSE factor; 3. The acquisition time for 3D FLAIR was 7 minutes 36 seconds. The parameters for 2D T2WI were the following: TR/TE, 3800/80 ms; turbo factor, 9; spatial resolution, 0.5 × 0.6 × 5 mm; SENSE factor, 2. The acquisition time for 2D T2WI was 3 minutes 56 seconds. The parameters for 2D FLAIR imaging were the following: TR/TE, 10,000/120 ms; turbo factor, 27; spatial resolution, 0.6 × 1.0 × 5 mm; SENSE factor, 1.2. The acquisition time for 2D FLAIR was 4 minutes. We performed DTI by single-shot echo-planar imaging. The parameters for DTI were the following: TE, 93 ms; spatial resolution, 1.8 × 1.8 × 2 mm; SENSE factor, 2.5. A maximum b-value of 1000 s/mm^2 in a 15-gradient-

direction technique was used with a SENSE factor of 2.5. The acquisition time for DTI was 5 minutes.

All images were parallel to the anterior/posterior commissure line. We created color maps from DTI datasets. The color-coding assumed that the eigenvector associated with the largest eigenvalue represents the average main fiber orientation of a particular pixel. In our color assignment, blue meant superior-inferior, green meant anteroposterior, and red meant laterolateral orientation. Tracts with oblique angles were represented by a mixture of colors.

Image Evaluation

All image assessment and measurement were performed on a PACS workstation. One experienced neuroradiologist evaluated the white matter tracts and nuclei of the brain stem on 3D and 2D FLAIR images and on 2D T2WI by referring to DTI color maps and the anatomic atlas.[6,8] The neuroradiologist selected the nuclei and white matter tracts that were identified as different colored areas on DTI color maps. The RN, SN, SCP, DSCP, and CST were consequently selected as the areas of interest at the midbrain; the SCP, CST, CTT, and MCP, at the pons.

Two neuroradiologists independently graded the visibility of the identified structures extracted on 3D and 2D FLAIR images and 2D T2WI by using a 4-point scale in which grade 0 indicated that the SI of the structure was lower than that of the adjacent white matter; grade 1, the SI of the structure was isointense to the adjacent white matter; grade 2, the SI of the structure was slightly higher than that of the adjacent white matter; and grade 3, the SI of the structure was much higher than that of the adjacent white matter. When the grades assigned by the 2 readers were different, the final grade was determined by consensus. The Wilcoxon signed-rank test was used to evaluate differences in the visibility of the identified structures on 3D and 2D FLAIR images and 2D T2WI.

For quantitative assessment, 1 neuroradiologist calculated the contrast ratio as the ratio of the difference in the SI of 2 structures (SI of the identified structure/SI of the adjacent white matter) identified on 3D and 2D FLAIR images and 2D T2WI. Regions of interest were placed on the basis of those images providing the best visibility of a given structure. These regions of interests were copied onto the 2 other image types. We measured the contrast ratio of a given structure on the right and left side and recorded the higher value as the contrast ratio of a given structure. For statistical analysis of our qualitative assessment results, we used the paired t test. A P value $<.05$ was considered statistically significant.

Results

Visibility and Statistical Analyses

A summary of the visibility of the identified structures of the brain stem on 3D and 2D FLAIR images and 2D T2WI is presented in Fig 1.

Midbrain. The 2 readers independently assigned the same grades for the RN, SN, DSCP, and CST on 3D FLAIR images of all volunteers; the consistency rate for the grade assigned to the SCP was 90%. On 2D FLAIR images, the assigned grades for the RN, SN, DSCP, and CST were also the same; the consistency rate of the grade assigned to the SCP was 80%. On 2D T2WI, the assigned grades for the RN, SN, SCP, DSCP, and CST were also the same for all volunteers. In all inconsistently graded cases, the difference was within 1 grade.

On consensus readings, grade 0 was assigned for the RN and SN in all volunteers on the 3 types of images (Figs 1*A* and 2*A*). The visibility of the CST was of grade 2 or 3 in all volunteers on 3D FLAIR images; there were no cases assigned grade 3 on 2D FLAIR images and 2D T2WI (Figs 1*A* and 2*A*). There was a statistically significant difference in the visibility of the CST on 3D and 2D FLAIR images ($P = .004$) and on 3D FLAIR images and 2D T2WI ($P = .002$). The visibility of the SCP and DSCP was grade 2 or 3 in all volunteers on 3D FLAIR images; grade 1 or 2 was assigned on 2D FLAIR images, and grade 1, on 2D T2WI (Figs 1*A* and 2*A*). There was a statistically significant difference in the visibility of the SCP and DSCP on 3D and 2D FLAIR images ($P = .002$ for SCP, $P = .005$ for DSCP) and on 3D FLAIR images and 2D T2WI ($P = .004$ for SCP, $P = .004$ for DSCP). There was no statistically significant difference between 2D FLAIR images and 2D T2WI.

Pons. The 2 readers independently assigned the same grades for the SCP and CTT on the 3D FLAIR images of all volunteers. The consistency rate for the grading of the MCP and CST was 90%. On 2D FLAIR images, the assigned grades for the MCP, CTT, and CST were the same; the consistency rate for the grading of the SCP was 80%. On 2D T2WI, the assigned grades for the SCP, MCP, and CTT were the same, and the consistency rate for grading of the CST was 90%. In all inconsistently graded cases, the difference was within 1 grade.

On consensus readings, the visibility of the CST was graded as 2 or 3 on 3D FLAIR images; on 2D FLAIR images and 2D T2WI, the assigned grade was 1 or 2 (Figs 1*B* and 2*B*). There was a statistically significant difference in the visibility of the CST on 3D and 2D FLAIR images ($P = .007$) and on 3D FLAIR images and 2D T2WI ($P = .005$) but not on 2D FLAIR images and 2D T2WI. The visibility of the SCP and CTT was grade 2 or 3; grade 1 or 2 was assigned to 2D FLAIR images, and grade 1, to 2D T2WI (Figs 1*B* and 2*B*). There was a statistically significant difference in the visibility of the SCP and CTT on 3D and 2D FLAIR images ($P = .011$ for the SCP, $P = .008$ for the CTT), on 3D FLAIR images and 2D T2WI ($P = .012$ for the SCP, $P = .003$ for the CTT), and on 2D FLAIR images and 2D T2WI ($P = .014$ for the SCP, $P = .025$ for the CTT). The visibility of the MCP was grade 2 or 3 in all but 1 subject on 3D FLAIR images; grade 1 or 2 was assigned on 2D FLAIR images and grade 1, on 2D T2WI in all subjects (Figs 1*B* and 2*B*). There was a statistically significant difference in the visibility of the MCP on 3D and 2D FLAIR images ($P = .003$) and on 3D FLAIR images and 2D T2WI ($P = .005$). There was no statistically significant difference between 2D FLAIR images and 2D T2WI.

Quantitative Statistical Analysis

The mean contrast ratio of each structure and the results of quantitative statistical analyses are shown in Tables 1 and 2 and Fig 3.

Midbrain. The contrast ratio for the CST, SCP, DSCP, RN, and SN was statistically different on 3D and 2D FLAIR images ($P = .0002$ for the CST, $P = .0014$ for the SCP, $P < .0001$ for the DSCP, $P = .047$ for the RN, and $P = .014$ for the SN) and on 3D FLAIR images and 2D T2WI ($P < .0001$ for the CST, $P = .0066$ for the SCP, $P < .0001$ for the DSCP, $P = .014$ for the RN, and $P = .0001$ for the SN). The mean contrast ratio of the CST, SCP, and DSCP was higher on 3D FLAIR images than on 2D FLAIR images and 2D T2WI (Fig 3*A*). The

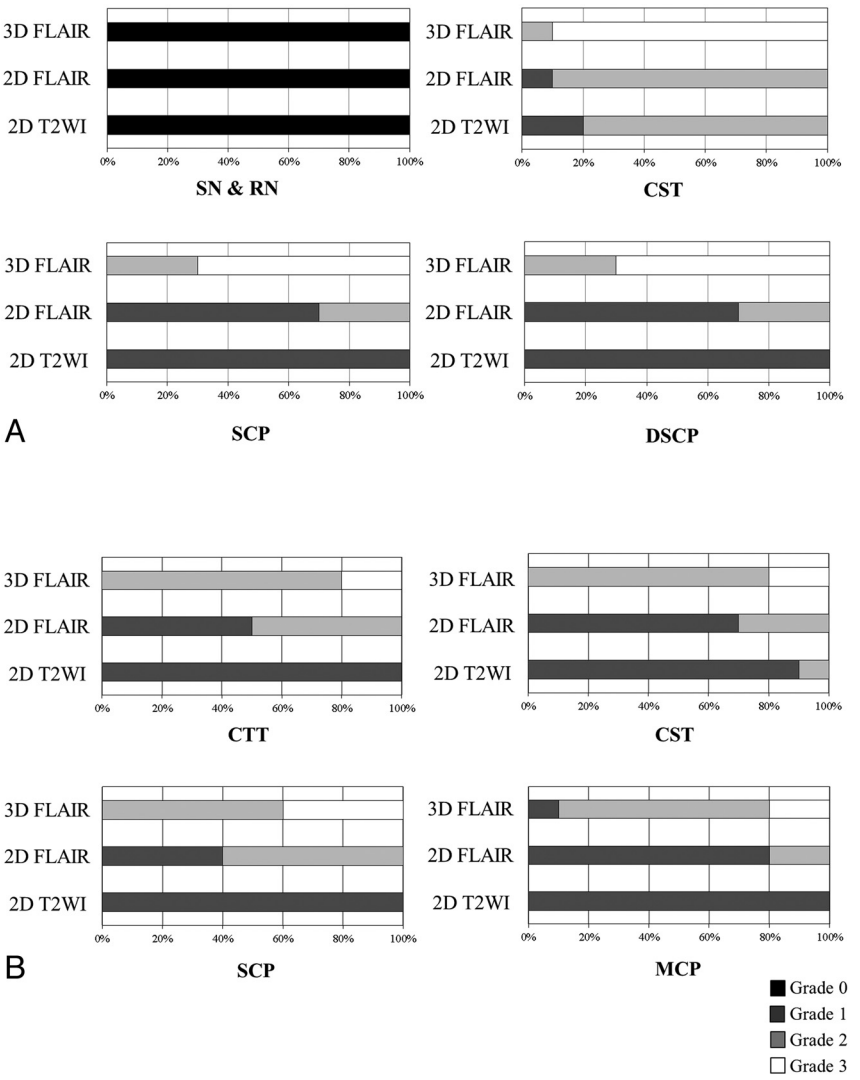

Fig 1. Visibility of identified structures. The percentage of each assigned grade on 3D and 2D FLAIR images and 2D T2WI. *A*, Bar graphs show the distribution of the assigned visibility grades for identified structures at the midbrain on 3D and 2D FLAIR images and 2D T2WI in all subjects. Grades 2 and 3 are more frequently assigned to the CST, SCP, and DSCP on 3D FLAIR than on 2D FLAIR images and 2D T2WI. *B*, Bar graphs show the distribution of the assigned visibility grades for identified structures at the pons on 3D and 2D FLAIR images and 2D T2WI in all subjects. Grades 2 and 3 are more frequently assigned to the CTT, CST, SCP, and MCP on 3D FLAIR than on 2D FLAIR images and 2D T2WI.

contrast ratio of the RN and SN was lower on 3D FLAIR images than on 2D FLAIR images and 2D T2WI.

Pons. There was a statistically significant difference in the contrast ratio for the CST, SCP, CTT, and MCP on 3D and 2D FLAIR images ($P = .0018$ for the CST, $P < .0001$ for the SCP, $P = .011$ for MCP, $P = .0024$ for CTT). The contrast ratio for the CST, CTT, and MCP was significantly different on 3D FLAIR images and 2D T2WI ($P = .0003$ for the CST, $P = .0062$ for the MCP, $P = .02$ for the CTT); the contrast ratio for the SCP was not. However, the contrast ratio for the SCP differed significantly on 2D FLAIR images and 2D T2WI ($P = .016$) (Fig 3*B*). The contrast ratio of the CST, CTT, and MCP was higher on 3D FLAIR images than on 2D FLAIR images and 2D T2WI.

Discussion

The complex anatomy of the brain stem includes a large number of tracts and nuclei, as well as multiple commissures and decussations. Our results indicate that 3D FLAIR images delineated white matter tracts with higher contrast than 2D FLAIR images and 2D T2WI. Gawne-Cain et al[9] reported that an increased signal intensity was seen in the CST in healthy volunteers on fast FLAIR images at 1.5T MR imaging. In our study, the CST exhibited the highest contrast on 3D FLAIR compared with 2D FLAIR images and 2D T2WI. Yagishita et al[10] demonstrated that the CST in the posterior limb of the internal capsule was hyperintense on T2WI and that large fibers with thick myelin sheaths produced the high signal intensity of the CST. The histologic characteristics reported by Yagishita et al[10] may affect the signal intensity of the CST on FLAIR images. According to Neema et al,[11] the CST manifested more prominent hyperintensity on 2D FLAIR images acquired at 3T than at 1.5T. We did not compare the data for 3D FLAIR between 3T and 1.5T; however, we believe that the higher signal intensity–to-noise ratio at 3T resulted in better delineation of the CST.

Some white matter structures other than the CST exhibited hyperintensity in our study. De Coene et al[12] demonstrated

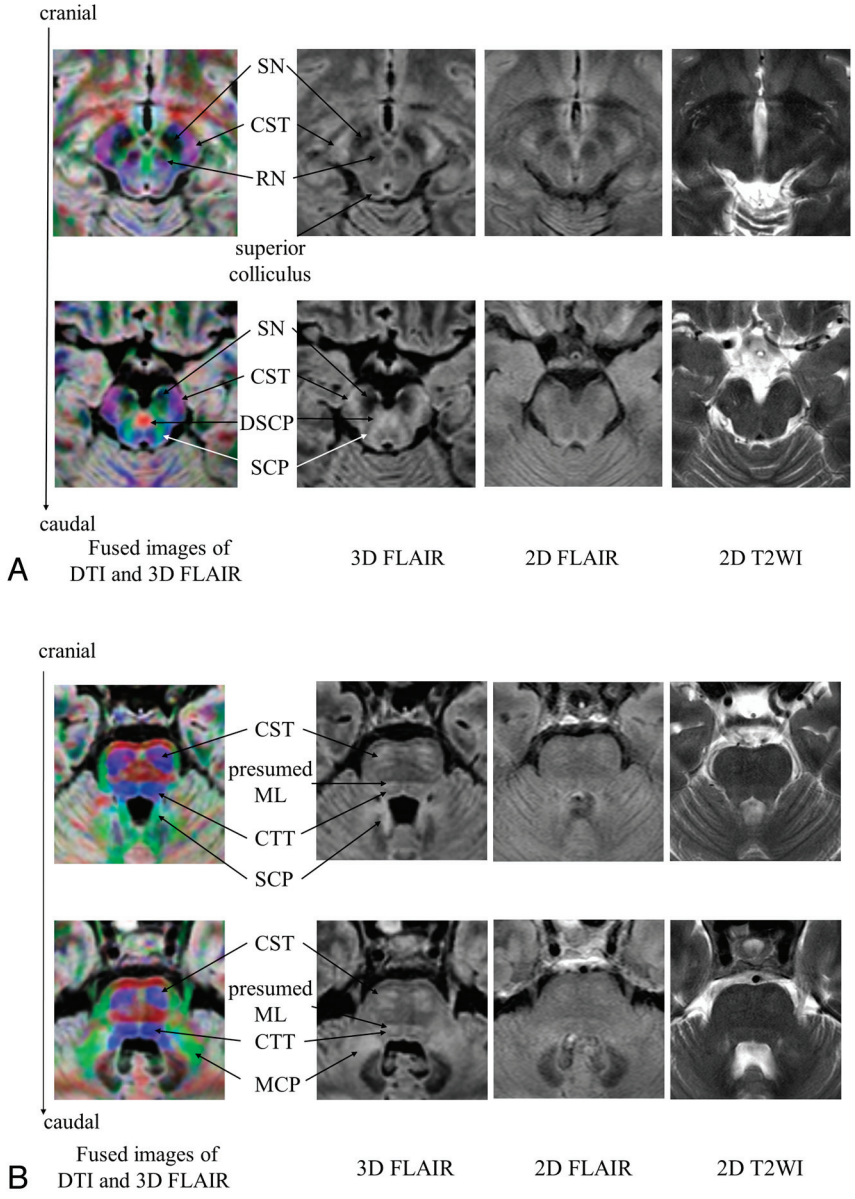

Fig 2. Midbrain and pontine anatomy. *A*, Midbrain: left column, fused images of 3D FLAIR and color maps; 2nd column from left, 3D FLAIR images; 3rd column, corresponding sections on 2D FLAIR images; right column, corresponding sections on 2D T2WI. Blue indicates superior-inferior orientation; green, anteroposterior orientation; red, laterolateral orientation. *B*, Pons: Left column, fused images of 3D FLAIR images and color maps; 2nd column from left, 3D FLAIR; 3rd column, corresponding sections on 2D FLAIR images; right column, corresponding sections on 2D T2WI. For color codes, see *A*.

Table 1: Mean contrast ratio of the anatomic structures on 3D and 2D FLAIR imaging and 2D T2WI in the midbrain

	SN Mean (SD)	RN Mean (SD)	CST Mean (SD)	SCP Mean (SD)	DSCP Mean (SD)
3D FLAIR	0.60 (0.07)	0.82 (0.10)	1.63 (0.09)	1.60 (0.10)	1.77 (0.08)
2D FLAIR	0.76 (0.03)	0.88 (0.06)	1.37 (0.12)	1.41 (0.07)	1.41 (0.08)
2D T2WI	0.80 (0.07)	0.93 (0.10)	1.34 (0.14)	1.38 (0.11)	1.37 (0.09)

that on heavily 2D FLAIR images, the white matter tracts in the brain stem including the CST, parietopontine tract, lateral lemniscus and ML, SCP, inferior cerebellar peduncle, DSCP, decussation of the inferior cerebellar peduncles, medial longitudinal fasciculi, thalamo-olivary tracts, and the cuneate and gracile fascicule exhibited a high signal intensity. We did not evaluate the visibility of the white matter tracts other than CST, DSCP, SCP, and MCP because we used DTI as the reference image. We did not evaluate some of the small white matter tracts (eg, the ML). Because the ML runs in a superior-inferior orientation in close vicinity to the CTT, it was difficult to differentiate the CTT and ML on DTI color maps. In careful comparison between the 3D FLAIR images and the anatomic atlas, ML on 3D FLAIR images seemed to exhibit high signal

Table 2: Mean contrast ratio of the anatomic structures on 3D and 2D FLAIR imaging and 2D T2WI in the pons

	CTT Mean (SD)	CST Mean (SD)	SCP Mean (SD)	MCP Mean (SD)
3D FLAIR	1.45 (0.16)	1.40 (0.18)	1.61 (0.11)	1.55 (0.20)
2D FLAIR	1.22 (0.05)	1.15 (0.04)	1.36 (0.07)	1.32 (0.10)
2D T2WI	1.21 (0.26)	1.13 (0.06)	1.50 (0.16)	1.24 (0.29)

intensity in close to vicinity to the CTT. Further studies are needed to clarify other small white matter tracts in the brain stem on 3D FLAIR images.

There are several explanations for the higher visibility and greater contrast of white matter tracts on 3D FLAIR images compared with 2D FLAIR sequences and 2D T2WI. First, the longer TE at 3D FLAIR compared with 2D T2WI and 2D FLAIR emphasizes the T2-weighted contrast effect. Second, 3D TSE with extended echo trains and variable low flip angles manifests a distinct diffusion sensitivity. Weigel and Henning[13] demonstrated that noticeable diffusion sensitivity accumulated along the echo train and that low refocusing flip angles created larger fractions of either well-dephased transversal or "stored" longitudinal magnetization on TSE sequences. Such spin behavior produced distinct diffusion sensitivity in the approximate range of $b = 80–100$ mm^2/s on 3D TSE sequences.

Third, the high turbo factor number of 3D FLAIR imaging may have affected the tissue contrast. In our study, the turbo factor for 3D FLAIR was much greater than that for 2D FLAIR imaging and 2D T2WI. The effect of the magnetization transfer contrast that depends on the number of turbo factors was different on 3D FLAIR imaging compared with 2D FLAIR imaging and 2D T2WI; this difference may have affected the 3D FLAIR contrast variation. Fourth, 3D FLAIR has fewer artifacts from vessels and CSF pulsation and less partial volume effect than 2D FLAIR and 2D T2WI,[4] and this may also contribute to the higher visibility and higher contrast of white matter tracts on 3D FLAIR images.

Regarding the visibility of the RN and SN, we found no statistically significant difference with respect to their visibility on the 3 types of images. Iron-containing tissues such as the RN and SN emit a low signal intensity; this is reflected in the increased susceptibility effects at longer TE values.

Our study involved a small number of neurologically healthy subjects. In individuals with brain stem lesions such as stroke, neoplasms, encephalitis, or multiple sclerosis, it is important to understand the relationship between the lesions and normal anatomic structures. Isotropic high-resolution 3D FLAIR images make it possible to delineate the relationship between the normal anatomic structures in the brain stem, yielding images that can be reformatted in any desired plane and facilitating the measurement of the lesion volume. 3D FLAIR images might be useful for the diagnosis and follow-up in patients with brain stem lesions. In the evaluation of brain stem lesions, some of the normal white matter tracts exhibit high intensity on 3D FLAIR images. Further studies are needed to clarify the usefulness of the 3D FLAIR sequence in patients with brain stem lesions. In this study, we did not evaluate the SI of the white matter tracts of the brain other than the brain stem. Further studies are needed to evaluate whether the white matter tracts of the brain other than the brain stem show high signal intensity on 3D FLAIR images.

Conclusions

3D FLAIR imaging can provide detailed anatomic information of the brain stem that cannot be obtained on conventional 2D FLAIR images and 2D T2WI. Our findings may help to

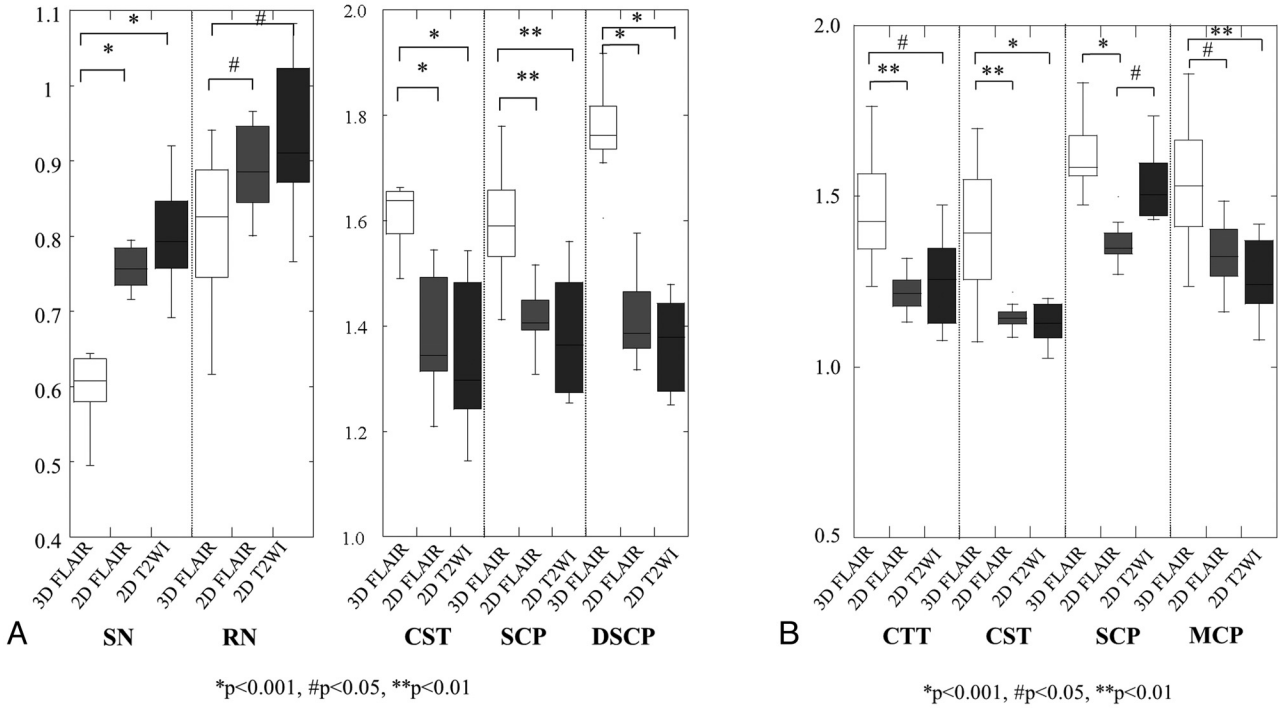

Fig 3. Statistical results for the contrast ratio of anatomic structures on 3D and 2D FLAIR images and 2D T2WI. *A,* Statistical results for the contrast ratio of anatomic structures on 3D and 2D FLAIR images and 2D T2WI at the midbrain. *B,* Statistical results for the contrast ratio of anatomic structures on 3D and 2D FLAIR images and 2D T2WI at the pons.

recognize signal-intensity abnormalities of the brain stem visualized on 3D FLAIR images.

References

1. Bink A, Schmitt M, Gaa J, et al. **Detection of lesion in multiple sclerosis by 2D FLAIR and single-slab 3D FLAIR sequence at 3.0 T: initial results.** *Eur Radiol* 2006;16:1104–10
2. Mike A, Glanz BI, Hildenbrand P, et al. **Identification and clinical impact of multiple sclerosis cortical lesions as assessed by routine 3T MR imaging.** *AJNR Am J Neuroradiol* 2011;32:515–21
3. Yamazaki M, Naganawa S, Kawai H, et al. **Increased signal intensity of the cochlea on pre-and post-contrast enhanced 3D-FLAIR in patients with vestibular schwannoma.** *Neuroradiology* 2009;12:855–63
4. Kallmes DF, Hui FK, Mugler JP 3rd. **Suppression of cerebrospinal fluid and blood flow artifacts in FLAIR MR imaging with a single-slab three-dimensional pulse sequence: initial experience.** *Radiology* 2001;221:251–55
5. Manova ES, Habib CA, Boikov AS, et al. **Characterizing the mesencephalon using susceptibility-weighted imaging.** *AJNR Am J Neuroradiol* 2009;30:569–74
6. Nagae-Poetscher LM, Jiang H, Wakana S, et al. **High-resolution diffusion tensor imaging of the brain stem at 3T.** *AJNR Am J Neuroradiol* 2004;25:1325–30
7. Mandelli ML, De Simone T, Minati L, et al. **Diffusion tensor imaging of spinocerebellar ataxias type 1 and 2.** *AJNR Am J Neuroradiol* 2007;28:1996–2000
8. Naidich TP, Duvernoy HM, Delman BN, et al. **Section VIII. Magnetic resonance microscopy at 9.4 Tesla: formalin-fixed human cadaver specimens.** In: Naidich TP, Duvernoy HM, Delman BN, et al. eds. *Duvernoy's Atlas of the Human Brain Stem and Cerebellum: High-Field MRI, Surface Anatomy, Internal Structure, Vascularization and 3D Section Anatomy.* Vienna, Austria: Springer-Verlag; 2009:247–414
9. Gawne-Cain ML, Silver NC, Moseley IF, et al. **Fast FLAIR of the brain: the range of appearances in normal subjects and its application to quantification of white matter disease.** *Neuroradiology* 1997;39:243–49
10. Yagishita A, Nakano I, Oda M, et al. **Location of the corticospinal tract in the internal capsule at MR imaging.** *Radiology* 1994;191:455–60
11. Neema M, Guss ZD, Stankiewicz JM, et al. **Normal findings on brain fluid-attenuated inversion recovery MR images at 3T.** *AJNR Am J Neuroradiol* 2009;30:911–16
12. De Coene B, Hajna JV, Pennock JM, et al. **MRI of the brain stem using fluid attenuated inversion recovery pulse sequence.** *Neuroradiology* 1993;35:327–31
13. Weigel M, Henning J. **On the diffusion sensitivity of 2D- and 3D-turbo spin sequences.** In: *Proceeding of the 19th Annual Meeting of the International Society for Magnetic Resonance in Medicine*, Montreal, Quebec, Canada. May 6–13, 2011